International Journal of Modern Physics B
Vol. 29, No. 5 (2015) 1550019 (8 pages)

DOI: 10.1142/S0217979215500198

Doping effect on the physical properties of $Li_xFe_{2-x}As$

W. Han*,†, X. C. Wang*, J. J. Gu†, Q. Q. Liu*, Z. Deng* and C. Q. Jin*,‡

*Institute of Physics, Chinese Academy of Sciences,
Beijing 100190, P. R. China
†Department of Physics, Hebei Normal University for Nationalities,
Chengde 067000, P. R. China
‡Jin@iphy.ac.cn

Received 2 May 2014
Revised 28 September 2014
Accepted 29 September 2014
Published 18 December 2014

We have studied the physical properties of Li-doped compound Fe_2As, which is isostructural to the famous iron-based superconductor LiFeAs. The results indicate that both a-axis and c-axis of $Li_xFe_{2-x}As$ increases with the increase in Li content when it is less than 0.2. The Néel temperature of $Li_xFe_{2-x}As$ decreases with the increase in Li content, which may be related to the changes of distance for Fe_{II}–Fe_{II} layers. The resistivity of $Li_xFe_{2-x}As$ is similar to that of Fe_2As at low doping level 0–0.2. As the doping amount is increased to 0.9, the resistivity of $Li_xFe_{2-x}As$ approaches the value of LiFeAs.

Keywords: 111-type superconductor; antiferromagnetic transition; $Li_xFe_{2-x}As$.

PACS numbers: 81.05.Bx, 75.50.Ee, 74.10.+v

1. Introduction

Since the discovery of the iron-based superconductor $LaFeAs(O_{1-x}F_x)$ with a superconducting transition temperature (Tc) of 26 K,[1] a series of new iron-based superconductors have been studied in succession.[2–10] All these iron-based superconductors crystallize into structures containing Fe–As layers where the superconductivity takes place. 111-type superconductors own a simple structure among the discovered superconductors, which makes them a suitable candidate for investigating the mechanism of iron-based superconductors. Fe_2As crystallizes into the same structure as 111-type iron-based superconductors, but with the Fe atom replaced by the alkaline metal as shown in Figs. 1(a) and 1(b). Hence, it is very interesting to investigate the doping effect of Li on the compound Fe_2As at the

‡Corresponding author.

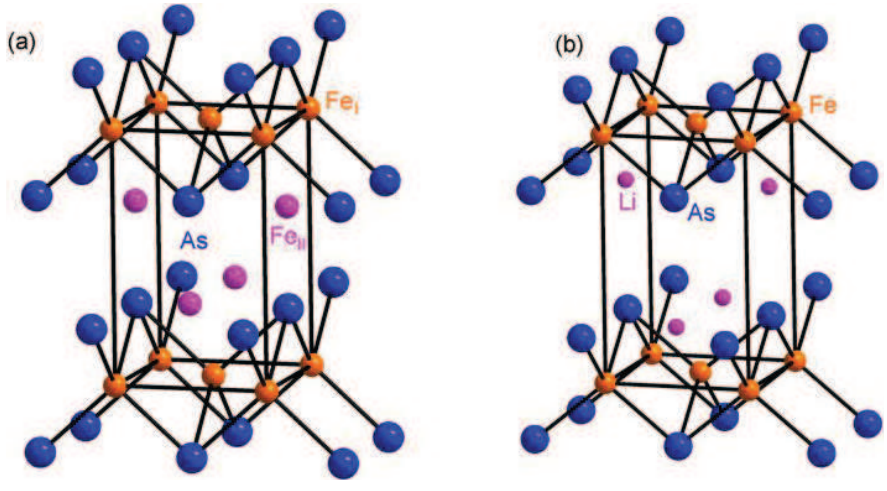

Fig. 1. (a) Crystal structures of tetragonal Fe_2As (antiferromegnet with $T_N \sim 356$ K), (b) crystal structures of tetragonal LiFeAs (nonmagnetic superconductor with $T_c \sim 16$ K).

Fe position between the Fe–As layers. Furthermore, it will be useful to reveal the mechanism of iron-based superconductors.

Fe_2As is antiferromagnetic and has a Néel temperature of about 356 K. Although Fe_2As, Mn_2As, Mn_2Sb and Cr_2As have Cu_2Sb-type crystal structure, their magnetic order is different.[11–13] The coupling between layers of iron atoms Fe_{II} located at (0, 1/2, z) and (1/2, 0, z) is antiparallel, but the coupling between a layer of iron atoms Fe_I located at (0, 0, 0) and (1/2, 1/2, 0) and adjacent Fe_{II} layers is parallel.[14] A number of experiments investigate magnetic properties of Fe_2As,[14–18] while there is very little work on the effect of Li-doped Fe_2As. In this paper, we study the doping effect of Li on the compound Fe_2As. It is found that both a- and c-axes expand with increasing Li content when it is less than 0.2, while no obvious changes occur when it is greater than 0.2. The $Li_xFe_{2-x}As$ compound is antiferromagnetic during the whole doping range, but the Néel temperature decreases with the increase in Li content. The resistivity shifts obviously to higher values with the doping amount of Li increasing from 0 to 1.0.

2. Experimental

The $Li_xFe_{2-x}As$ compound was synthesized using solid state reaction method. The Li_3As precursor was synthesized from the mixtures of high-purity Li granular plus arsenic powder sealed into an evacuated quartz tube that are sintered at 650°C for 30 h. Here we address that using Li_3As precursors instead of Li elements helps much to achieve homogenous reaction with increasing Li contents because the alkaline or alkaline earth metals are very volatile at high temperature. The initial stoichiometric composition of Li_3As, As and high-purity Fe powders were mixed according to nominal composition $Li_xFe_{2-x}As$. The mixtures were sealed into an

evacuated titanium tube, and then it was heated to 800°C at 3°C/min, and kept for 30 h before slowly decreasing to room temperature at a rate of 2°C/min. The sintered materials were ground, then the previous reaction process was repeated in order to make homogeneous samples. The recovered samples were characterized by X-ray powder diffraction (XRD) with a Philips X'pert diffractometer using CuK_1 radiation. Diffraction data were collected with 0.02° and 15 s/step. Rietveld analysis was performed by using the GSAS program software package.[19] The DC magnetic susceptibility was measured using an SQUID magnetometer (Quantum Design) and the electrical resistivity for sintered pellet samples was examined by a physical property measurement system (Quantum Design).

3. Results and Discussion

Figures 2(a) and 2(b) show the XRD pattern of sample with nominal composition $Li_xFe_{2-x}As$. It can be seen that all these diffraction patterns can be indexed into

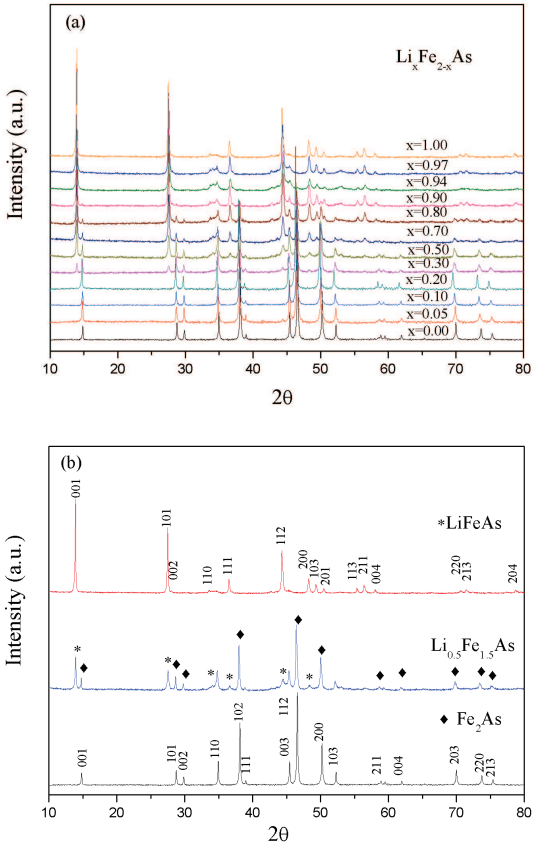

Fig. 2. Powder XRD of $Li_xFe_{2-x}As$ (x = 0, 0.05, 0.10, 0.20, 0.30, 0.50, 0.70, 0.80, 0.90, 0.94, 0.97, 1.00). The symbols ∗ and ♦ denote the phases Fe_2As and LiFeAs, respectively.

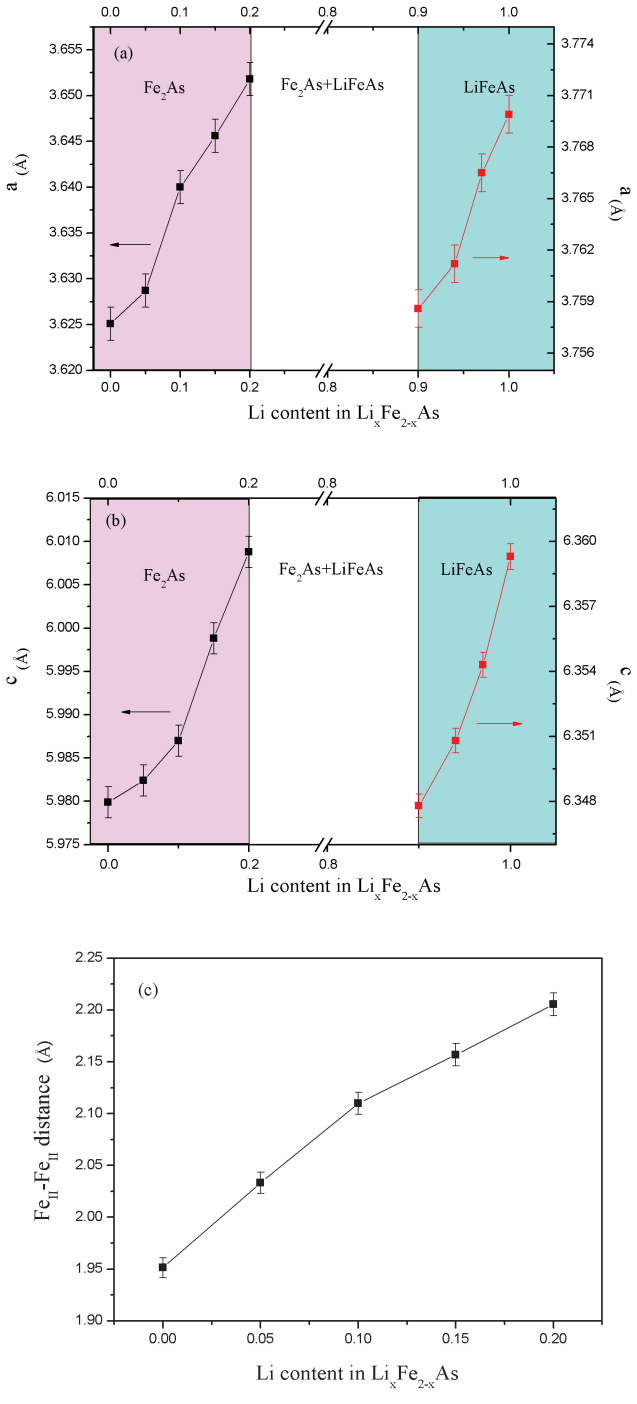

Fig. 3. (a) and (b) Lattice parameters for $Li_xFe_{2-x}As$, (c) the evolution of distance of Fe_{II} layer for $Li_xFe_{2-x}As$ as a function of the Li content.

the tetragonal structure with the space group *P4/nmm* when x is smaller than 0.2, which is similar to Fe_2As as shown in Fig. 2(b). With the increasing Li content, it is observed that the (001), (101), (002), (110), (111), (112), (200), and (211) peaks of LiFeAs appeared in the XRD pattern together with Fe_2As structure, which is similar to $Li_{0.5}Fe_{1.5}As$ shown in Fig. 2(b). This means that the structure of $Li_xFe_{2-x}As$ is formed by Fe_2As and LiFeAs in a range of x from 0.3 to 0.9. As to the 0.9 doping, the (001), (101), (002), (110), (102), (112), (200) and (103) peaks of Fe_2As disappeared in the XRD pattern. These diffraction patterns can be indexed into the LiFeAs structure for $x > 0.9$. Figures 3(a) and 3(b) show the evolution of lattice parameters for $Li_xFe_{2-x}As$ as a function of the Li content. The lattice parameters are refined based on a *P4/nmm* space group by a least-squares fit using at least 10 XRD peaks. Both a-axis and c-axis gradually expand with the Li content increasing in $Li_xFe_{2-x}As$ compared with the parent compound Fe_2As. Fe_2As and LiFeAs have the same space group and Fe–As layers, while the lattice parameters for LiFeAs are $a = 3.6518$ Å and $c = 6.0088$ Å, which are larger than Fe_2As.[10] Their differences lie in iron atoms Fe_{II} and lithium atom in different positions. The lattice constants increase in the doping level 0–0.2 and 0.9–1.0, which may be due to the fact that the structure of $Li_xFe_{2-x}As$ gradually approaches the structure of LiFeAs. Figure 3(c) shows the evolution of distance of Fe_{II} layer as a function of the Li content, obtained from the result of refinement. Compared with the parent compound Fe_2As, the distance of Fe_{II} layer gradually expands with increasing content of Li in $Li_xFe_{2-x}As$.

Figures 4(a) and 4(b) show the magnetization measurements of $Li_xFe_{2-x}As$ in field-cooled (FC) mode at 30 Oe, indicating a very sharp antiferromagnetic transition at 356 K for Fe_2As. This agrees with the neutron diffraction result,[14] while the antiferromagnetic transition temperature is 293 K for $Li_{0.2}Fe_{1.8}As$. Below the Néel temperature, the magnetic susceptibility first increases and then slightly decreases with decreasing temperature, which is consistent with others.[12] The magnetic susceptibility above the Néel temperature for $Li_{0.2}Fe_{1.8}As$ obeys the Curie–Weiss law as follows: $\chi = 2.91/(T - 170.1)$ emu/mol. The effective Bohr magneton per iron atom is estimated to be 3.59 μ_B on the average of the two sublattices which are smaller than Fe_2As (4.66 μ_B).[14] The inset of Fig. 4(b) shows that the superconducting transition at 16 K is clearly observed for samples of nominal composition LiFeAs, which agrees with the results in Ref. 10. Figure 4(c) shows the Néel temperature (T_N) for $Li_xFe_{2-x}As$ with x being smaller than 0.2. It decreases with increasing content of Li in $Li_xFe_{2-x}As$. We also find that the distance of Fe_{II} layer gradually expands, accompanied by the decrease in T_N with increasing content of Li in $Li_xFe_{2-x}As$. Combining the changes in T_N for $Li_xFe_{2-x}As$ with the evolution of distance for Fe_{II} layers, we find that the antiferromagnetic coupling between layers of iron atoms Fe_{II} becomes weaker, while the distance for Fe_{II} layers expands. Thus, we can conclude that the decrease in T_N may be related to the changes in distance for Fe_{II} layer.

In order to investigate the correlation between the Li content of $Li_xFe_{2-x}As$ and resistivity of polycrystalline specimens, zero-field electrical resistivity was measured

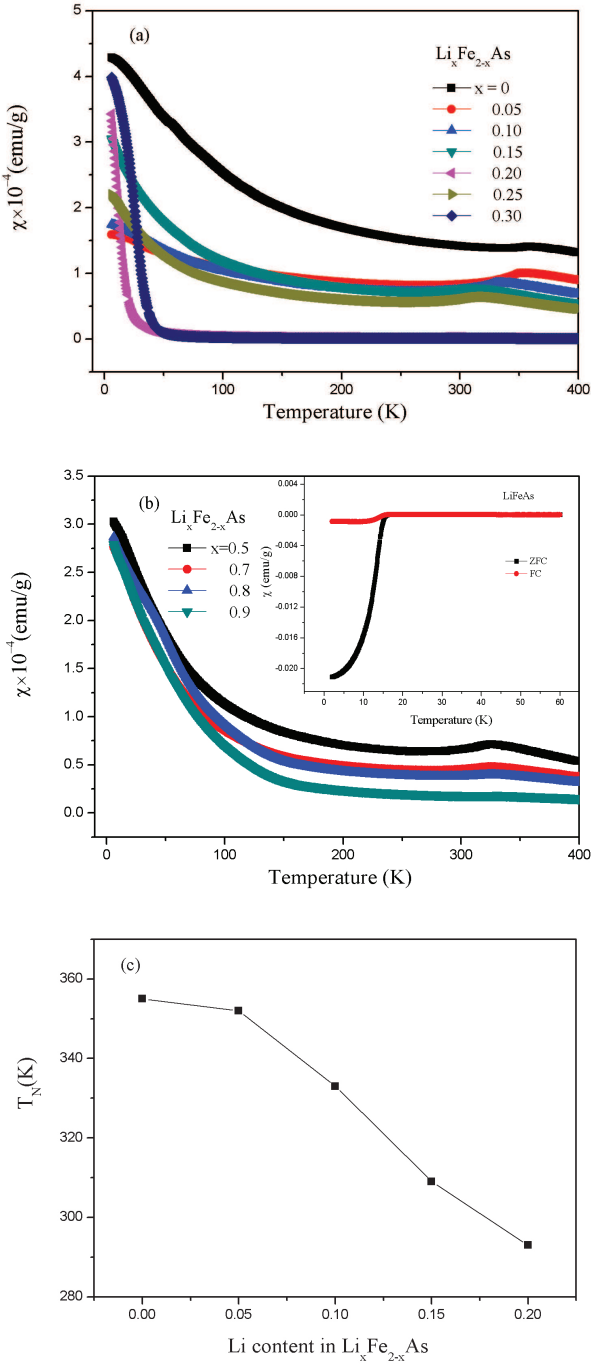

Fig. 4. Temperature dependence of susceptibility in field-cooled (FC) forms for (a) $0 \leq x \leq 0.3$ and (b) $0.5 \leq x \leq 1.0$ in the $Li_xFe_{2-x}As$ family at 30 Oe, (c) The Néel temperature for $Li_xFe_{2-x}As$.

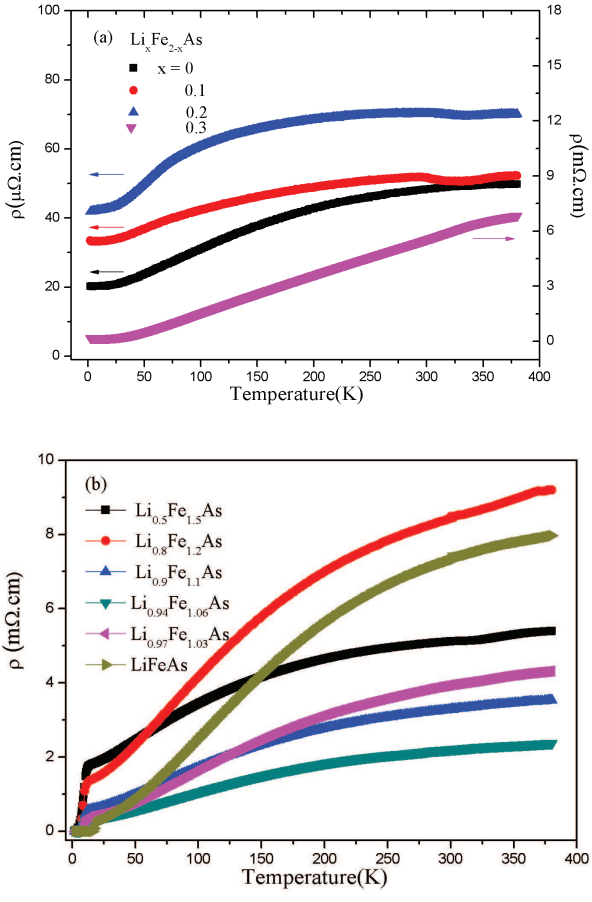

Fig. 5. Temperature dependence of the resistivity at ambient and 0 T for (a) $0 \leq x \leq 0.3$ and (b) $0.5 \leq x \leq 1.0$ in the $Li_xFe_{2-x}As$ family.

by using a physical property measurement system. Figures 5(a) and 5(b) show the resistivity of polycrystalline specimens of $Li_xFe_{2-x}As$, which was measured from 2 K to 380 K using a conventional four-probe method. The electric resistivity of Fe_2As is $\sim 10^{-5}$ ohm cm, in good agreement with the reported result.[18] One can see that the resistivity of $Li_xFe_{2-x}As$ shifts obviously to higher values with the doping amount of Li changing from 0 to 0.2. When x is larger than 0.3, the value of $Li_xFe_{2-x}As$ is up to $\sim 10^{-3}$ ohm cm, which approaches the value of LiFeAs.[10] The above phenomenon may originate from the electronic structure. The formal charge balance, $Li^{+1}Fe^{+2}As^{-3}$, leaves an average charge of -1 per Fe-As pair, similar to the undoped, nonsuperconducting 1111-type and 122-type.[20] The atom of Fe_{II} in Fe_2As, which is similar to Li in LiFeAs, presents +1, while Fe_I presents +2. Thus, Fe_{II} has the electronic structure of $3d^64s^1$. It is obvious to conclude that the Fe_{II} 4s electron is itinerant, resulted in the resistivity for $Li_xFe_{2-x}As$ smaller than LiFeAs.

4. Summary

In this work, we discover some interesting results by replacing part of iron atoms Fe_{II} with Li. It is found that: both a-axis and c-axis expand with increasing content of Li in the doping level 0–0.2 and 0.9–1.0. The Néel temperature for $Li_xFe_{2-x}As$ decreases with increasing content of Li, which may be related to the changes in distance for Fe_{II} layer. At low doping level 0–0.2 the resistivity of $Li_xFe_{2-x}As$ is similar to that Fe_2As. As the doping amount is increased to 0.9, the resistivity of $Li_xFe_{2-x}As$ approaches the value of LiFeAs.

Acknowledgments

This work was supported by NSF & MOST of China through research projects.

References

1. Y. Kamihara *et al.*, *J. Am. Chem. Soc.* **130**, 3296 (2008).
2. X. H. Chen *et al.*, *Nature* **453**, 761 (2008).
3. G. F. Chen *et al.*, *Phys. Rev. Lett.* **100**, 247002 (2008).
4. Z.-A. Ren *et al.*, *Euro. Phys. Lett.* **82**, 57002 (2008).
5. H. H. Wen *et al.*, *Euro. Phys. Lett.* **82**, 17009 (2008).
6. M. Rotter, M. Tegel and D. Johrendt, *Phys. Rev. Lett.* **101**, 107006 (2008).
7. F.-C. Hsu, *Proc. Natl Acad. Sci. USA* **105**, 14262 (2008).
8. X. Dai *et al.*, *Phys. Rev. Lett.* **101**, 057008 (2008).
9. C. de la Cruz *et al.*, *Nature* **453**, 899 (2008).
10. X. C. Wang *et al.*, *Solid State Commun.* **148**, 538 (2008).
11. A. E. Austin, E. Adelson and W. H. Cloud, *J. Appl. Phys.* **33**, 1356S (1962).
12. M. K. Wilkinson, N. S. Gingrich and C. G. Shull, *J. Phys. Chem. Solids* **2**, 289 (1957).
13. H. Watanabe, Y. Nakagawa and K. Sato, *J. Phys. Soc. Jpn.* **20**, 2244 (1965).
14. H. Katsuraki and N. Achiwa, *J. Phys. Soc. Jpn.* **21**, 2238 (1966).
15. N. Achiwa *et al.*, *J. Phys .Soc. Jpn.* **22**, 2238 (1967).
16. P. Raj and S. K. Kulshreshtha, *Phys. Scri.* **14**, 125 (1976).
17. L. M. Corliss *et al.*, *Phys. Rev. B* **25**, 245 (1981).
18. Y. Hwang *et al.*, *J. Appl. Phys.* **105**, 07A946 (2009).
19. A. C. Larson and R. B. Von Dreele, *Los Alamos Natl. Lab. [Rep.] LA* (*US*) LAUR 86-748 (1994).
20. M. Gooch *et al.*, *Euro. Phys. Lett.* **85**, 27005 (2009).